

Antitumor Activity of FL118, a Survivin, Mcl-1, XIAP, and cIAP2 Selective Inhibitor, Is Highly Dependent on Its Primary Structure and Steric Configuration

Jiuyang Zhao,[†] Xiang Ling,[‡] Shousong Cao,[§] Xiaojun Liu,[‡] Shengbiao Wan,[†] Tao Jiang,^{*,†} and Fengzhi Li^{*,‡,||}

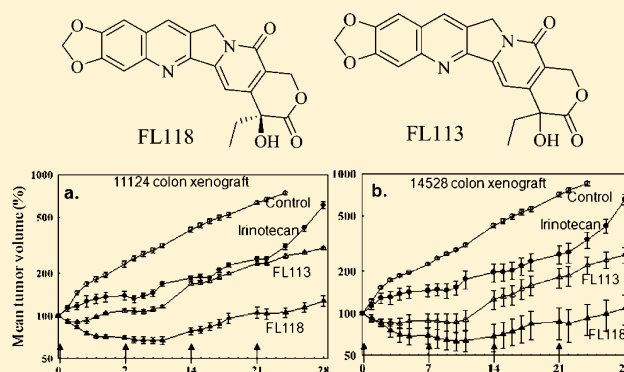
[†]Key Laboratory of Marine Drugs, Ministry of Education of China, School of Medicine and Pharmacy, Ocean University of China, 5 Yushan Road, Qingdao, Shandong 266003 China

[‡]Departments of Pharmacology & Therapeutics and [§]Medicine and ^{||}NCI-Supported Experimental Therapeutics Program, Roswell Park Cancer Institute, Elm and Carlton Streets, Buffalo, New York 14263, United States

Supporting Information

ABSTRACT: We recently reported the identification and characterization of a novel small chemical molecule designated FL118. FL118 selectively inhibits multiple cancer survival and proliferation-associated antiapoptotic proteins (survivin, Mcl-1, XIAP, cIAP2) and eliminates small and large human tumor xenografts in animal models (Ling et al., *PLoS One* 2012, 7, e45571). Here, we report a follow-up study on the structure–activity relationship (SAR) of the hydroxyl group in the lactone ring of FL118. We found that the superior antitumor efficacy of FL118 heavily depends on its steric configuration through comparing the antitumor activity of FL118 with FL113 (the racemic mixture of FL118). Consistently, FL118 proved much more effective in inhibiting the expression of survivin, Mcl-1, and cIAP2, both *in vitro* and *in vivo*, compared to FL113. Additionally, Tet-on controlled induction of survivin or forced expression of Mcl-1 protects cancer cells from FL118-mediated growth inhibition and cell death. To further explore the SAR, we synthesized seven position 20-esterifiable FL118 and FL113 derivatives. Studies on these seven new compounds revealed that keeping a free hydroxyl group of FL118 is also important for high antitumor efficacy. Together, these studies confirm the superior anticancer activity of FL118 and narrow the window for further SAR studies to generate novel analogues based on FL118 core structure on its other potential chemical positions.

KEYWORDS: IAP inhibitor, FL118, camptothecin analogue, SAR analysis, human tumor animal models, cancer cells



1. INTRODUCTION

Studies of the inhibitor of apoptosis (IAP) protein survivin and its gene in the literature have revealed its important role in anticancer drug resistance and cancer progression.^{1–12} We have established and validated genetically modified cancer cell models in which the luciferase reporter gene was driven under the human survivin gene regulatory sequences including the untranslated regulatory sequences of survivin mRNA.¹³ Using this assay system via high throughput screening of chemical compound libraries, followed by *in vitro* and *in vivo* testing, we finally identified one small chemical molecule designated FL118 (Figure 1) which possesses superior antitumor activity in animal models of human tumors.¹⁴ Interestingly, while FL118 (NSC634724) structurally is similar to camptothecin (Figure 1) and was considered as a camptothecin analogue,¹⁵ FL118 is actually an IAP inhibitor and shows poor ability to inhibit topoisomerase 1 (Top1) activity in comparison with SN-38, the active form/metabolite of irinotecan¹⁴ (Figure 1). We previously demonstrated that FL118 selectively inhibits the expression of

survivin, Mcl-1, XIAP, and cIAP2.¹⁴ In this regard, not only survivin,^{1–12} but also XIAP,^{16–21} cIAP2,^{22,23} and Mcl-1,^{24–31} are involved in anticancer drug resistance and/or prognostic/diagnostic values in various types of cancer.

The exceptional *in vivo* antitumor activity of FL118 has not been recognized until our recent report which demonstrates that FL118 shows superior and broad antitumor efficacy.¹⁴ This suggests that FL118 would be a great core structure for generation of new FL118 analogs. As an additional piece of evidence, our recent studies revealed that FL118, in an intravenous (i.v.) compatible formulation, further decreases its toxicity to animals and increases its therapeutic index (TI).³² We hope that, through studies assessing the structure–activity relationship (SAR) between FL118 and its close structurally

Received: July 25, 2013

Revised: October 31, 2013

Accepted: December 15, 2013

Published: December 15, 2013

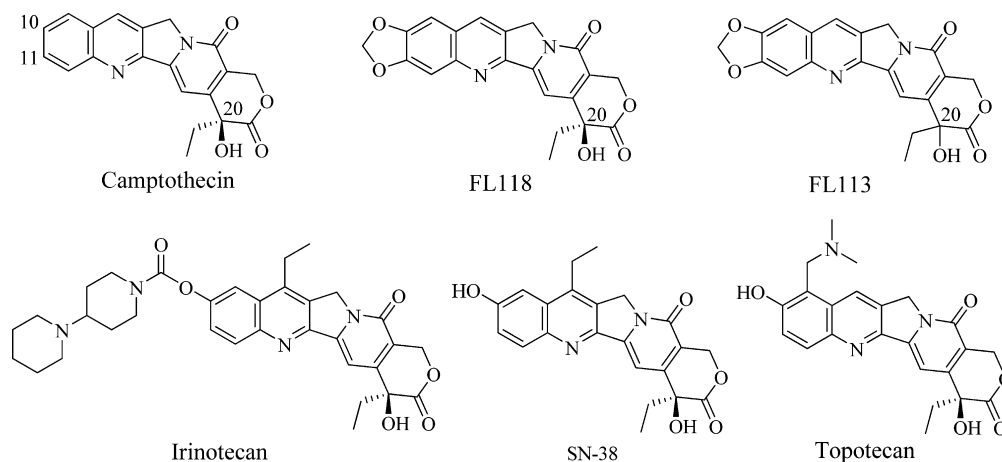


Figure 1. Structure of camptothecin, FL118, FL113, irinotecan, SN-38 (the active form of irinotecan), and topotecan.

related analogues, we will be able to obtain overall better anticancer molecules that are highly relevant to the FL118 structure but show an improved TI without increasing adverse toxicity to normal tissues. Previous studies indicated that the 10,11-methylenedioxcamptothecin (10,11-MDC or FL113) (Figure 1) exhibits high antitumor activity.³³ In the present study, we first compared the antitumor activity between FL113 (NSC606174) and its S-configuration, FL118 (NSC634724). We found that the superior antitumor efficacy of FL118 is highly dependent on the steric configuration of its hydroxyl group in the lactone ring (Figure 1), since antitumor activity of FL113 is much weaker than FL118. We then synthesized seven position 20-esterifiable FL113 and FL118 derivatives for comparison and found that keeping a free hydroxyl group is also important for high antitumor efficacy.

2. CHEMISTRY

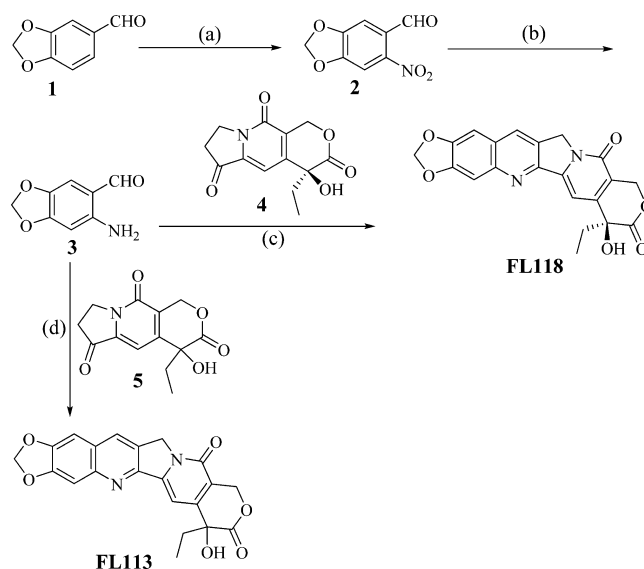
According to published procedures, 2-amino-4,5-methylenedioxybenzaldehyde **3** was prepared from piperonal **1** by nitration and reduction.^{34,35} The synthesis of FL118 and FL113 was accomplished using a Friedlander condensation between compound **3** and the known tricyclic keto lactone **4** and **5**, respectively^{36,37} (Scheme 1).

Coupling of compound FL113 and FL118 with substituted benzoic acids **6**, catalyzed by EDCI and DMAP, resulted in position 20-esterifiable FL113 derivatives **7a**, **7f**, **7g**, and FL118 derivatives **7b**–**7e** (Scheme 2).

3. RESULTS AND DISCUSSION

3.1. Superior Antitumor Activity of FL118 Heavily Depends on Its Steric Configuration. We previously showed that FL118 is highly effective in inhibiting human head-and-neck and colon tumors in animal xenograft models.¹⁴ Through comparison of antitumor potential among 16 chemical structurally relevant FL118 analogues (Supplemental Table S1), we found that FL113 and FL118 are the top two compounds showing the highest anticancer potential. To further study the SAR for compounds that are structurally highly relevant to FL118, we first compared the antitumor activity between FL118 and FL113 in human tumor animal models. Our studies indicated that FL118 and its racemic mixture FL113 showed better antitumor activity at their sub-MTD (maximum tolerated dose) level [1 mg/kg, of note FL113/118 MTD is ~1.5 mg/kg in weekly (wk) × 4 schedules¹⁴] than irinotecan (a camptothecin

Scheme 1. Synthesis of Compound FL118 and FL113^a



^aReagents and conditions: (a) HNO₃, 2–5 °C, 4 h, 68%; (b) FeSO₄·7H₂O, NH₄OH, EtOH/H₂O, 0.5 h, 71%; (c) *p*-TsOH, toluene, reflux, 12 h, 65%; (d) *p*-TsOH, toluene, reflux, 12 h, 67%.

analog structurally relevant to FL118, Figure 1) at its MTD level (100 mg/kg, weekly × 4) in two human colon tumor xenografts directly established from patients' colon cancer tissues. However, FL118 showed strikingly better antitumor activity than FL113 (Figure 2). This indicates that the compound with an R configuration likely has a much weaker antitumor activity than the compound with an S configuration for the “–OH” group at the 20-position. This finding is consistent with an earlier finding that the activity of camptothecin analogs is highly chemical structurally dependent.³⁸

FL118, FL113, and irinotecan are structurally related camptothecin analogues. Early studies demonstrated that camptothecin inhibits the synthesis of DNA,³⁹ RNA,⁴⁰ and protein,⁴¹ which was later found to be due to inhibition of DNA topoisomerase 1 (Top1) activity.^{42,43} As a proof, certain Top1 mutants in cancer cells produced resistance to camptothecin.⁴⁴ For example, the functional activity for irinotecan or topotecan is unexceptionally linked to inhibiting DNA Top1 activity as a major mechanism of action (MOA).^{45–49} Our previous studies showed that FL118 greatly exhibits superior antitumor efficacy in

Scheme 2. Synthesis of Compound 7a–7g

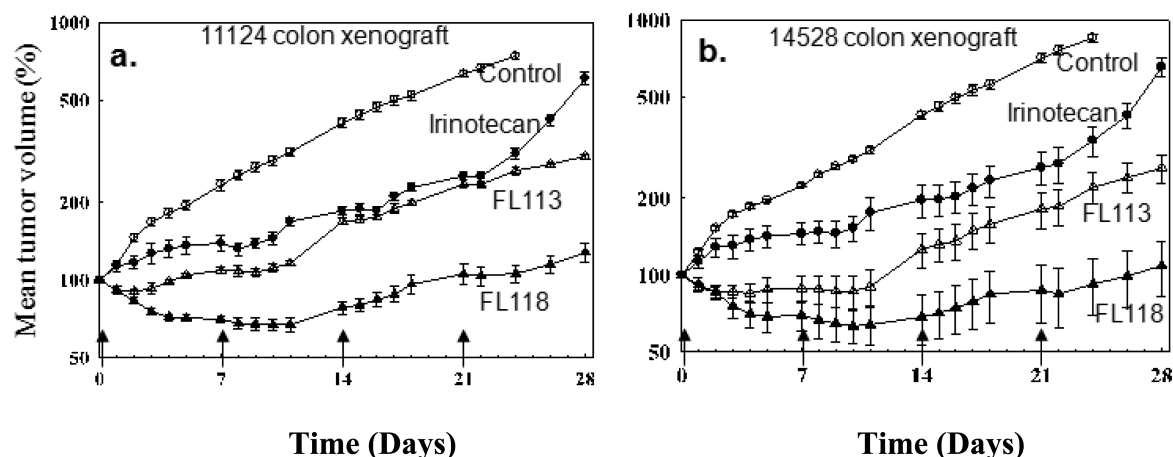
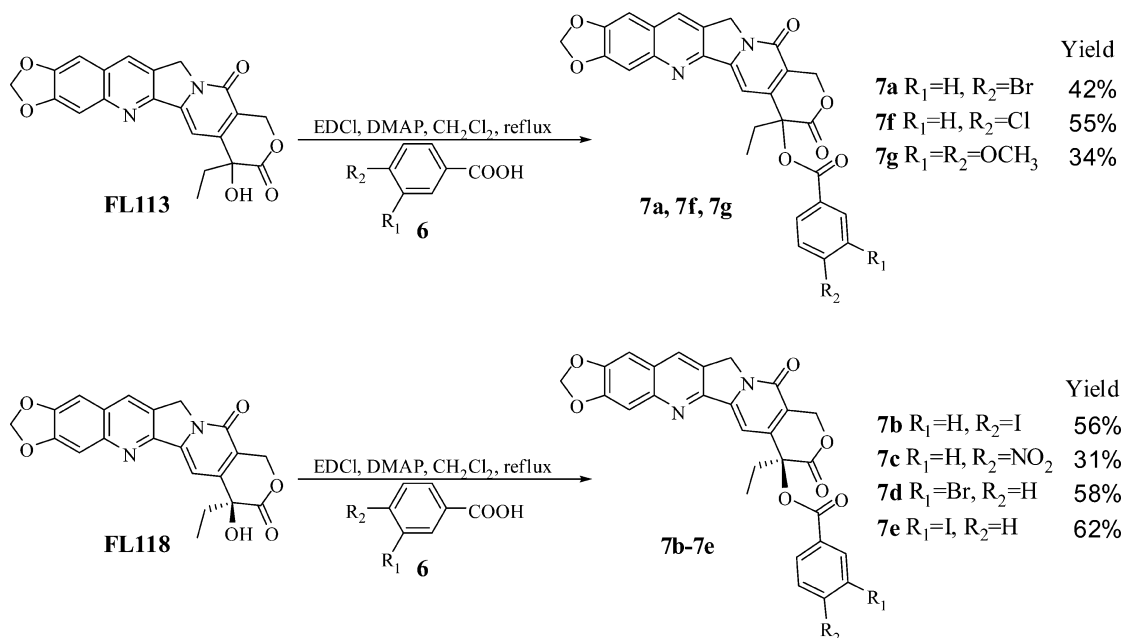


Figure 2. Comparison of the *in vivo* antitumor efficacy among FL113, FL118, and irinotecan (CPT-11): The SCID mouse models of human colon cancer xenografts were used to evaluate the relative antitumor activity for FL113 and FL118 versus irinotecan (control). Two human primary colon cancer xenografts 11124 (a) and 14528 (b), which were originally isolated from anonymous colon cancer patients, were first established in SCID mice and then used in the experiment. Drug treatment was conducted with the clinically relevant schedule of irinotecan (weekly \times 4) indicated by the arrows. The initial drug treatment was designated Day 0, and the treatment was initiated 7 days post subcutaneous tumor implantation, on which tumor size is about 200–250 mm³. The tumor curve in each treatment condition is the mean \pm SE derived from five individual tumors on five mice. Doses: irinotecan, 100 mg/kg per dose; FL113, 1.0 mg/kg per dose; and FL118, 1.0 mg/kg per dose.

comparison with irinotecan and topotecan.¹⁴ However, FL118 only showed about half of the Top1 inhibition ability of SN-38, the active metabolite of irinotecan, at the highest concentration (1 μ M) that can be reached by irinotecan *in vivo*.¹⁴ Moreover, in contrast to the weak inhibitory effects of FL118 on Top1 activity at a dose as high as 1 μ M, FL118 effectively initiated cancer cell apoptosis and the inhibition of survivin promoter activity, surviving expression, and cancer cell growth at 0.1 nM to 10 nM levels,¹⁴ indicating that the inhibition of Top1 activity by FL118 may not play a major role in its antitumor activity, apoptosis induction, and cancer cell growth inhibition.

3.2. FL118 Exhibits a High Ability To Eradicate Human Tumors in Animal Models at a Sub-MTD Dose. To confirm the antitumor efficacy of FL118 at its sub-MTD condition (<1.5 mg/kg), we used the human head-and-neck cancer cell line

FaDu-established tumor xenograft animal model to further explore its potential. Our data revealed that, while the tumors in the control group ($n = 10$) treated with the vehicle reached their maximal sizes allowed by Institutional Animal and Care Use Committee (IACUC) regulations (≤ 2000 mm³) within two weeks (Figure 3a), the tumors in the experimental groups ($n = 10$ per group) treated with FL118 at its sub-MTD (1 mg/kg and 1.25 mg/kg) with the weekly \times 4 schedule resulted in tumor eradication without relapse in a high percentage of mice (Figure 3b, c). Specifically, FL118 eliminated 6 out of 10 tumors in mice at 1 mg/kg with weekly \times 4 schedules (Figure 3b); and 7 out of 10 tumors in mice at 1.25 mg/kg with weekly \times 4 schedules (Figure 3c). Additionally, favorable results were also obtained using the human colon SW620 cancer cell line-derived tumor xenograft (Figure 3d, e, f).

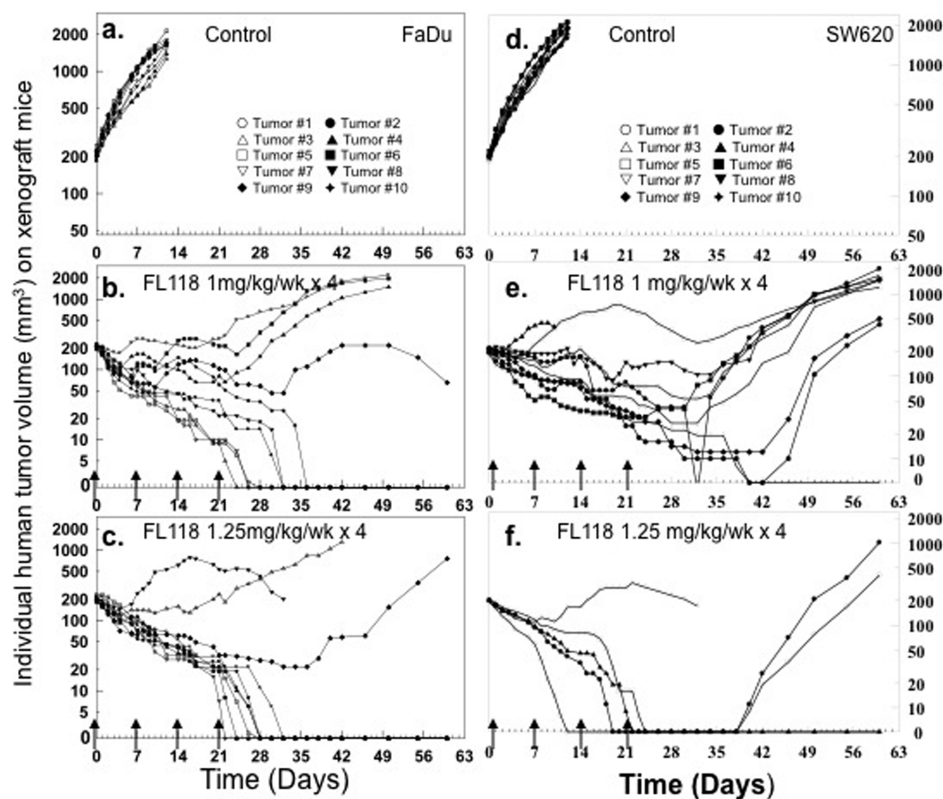


Figure 3. Antitumor activity of FL118 at its sub-MTD: FL118 treatment (designated Day 0, weekly $\times 4$, indicated with arrows) initiated 7 days after subcutaneous tumor implantation, when individual tumors grew to $\sim 200\text{--}250\text{ mm}^3$. (a, b, and c) Antitumor activity of FL118 at its sub-MTD (its MTD: 1.5 mg/kg weekly $\times 4$). Antitumor activity of FL118 in individual mice ($N = 10$ per group) at the dose of 1 mg/kg (b) and 1.25 mg/kg (c) versus the vehicle control (a) in mice bearing human FaDu head and neck tumor xenografts is shown. (d, e, and f) Antitumor activity of FL118 in individual mice at the dose of 1 mg/kg (e) and 1.25 mg/kg (f) versus the vehicle control (d) in mice bearing human SW620 tumor xenografts is shown.

Our results showed that FL118 treatment at its MTD (1.5 mg/kg, weekly $\times 4$) eradicates up to 100% human tumors in animal models using a human primary head-and-neck cancer tissue-established xenograft tumor.¹⁴ Here, our new data revealed that a significant percentage of tumors could be eliminated by FL118 even at a dose under its MTD (Figure 3).

3.3. FL118 Appears To Be a Much Better Compound to Inhibit Its Downstream Targets than FL113 *in Vitro* and *in Vivo*. Our previous studies revealed that, consistent with its superior antitumor activity, FL118 selectively inhibits multiple cancer cell survival and proliferation-associated antiapoptotic proteins including survivin, Mcl-1, XIAP, and cIAP2.¹⁴ To determine the possibility that the lower efficacy of FL113 in antitumor activity in comparison with FL118 (Figure 2) is due to the lower effectiveness of FL113 in the downregulation of FL118 targets (survivin, Mcl-1, XIAP, and cIAP2), human head-and-neck FaDu cancer cells were treated with and without FL113 (10 nM) or FL118 (10 nM) for 48, 72, and 96 h, followed by determining FL118 target protein expression using Western blots. The results showed that FL118 appears to be much more effective in inhibiting these protein targets (Figure 4). To further investigate whether FL113 and FL118 treatment could display similar results as observed *in vitro* using cultured cancer cells (Figure 4a), we collected human FaDu tumor tissues from xenograft mice 72 h post FL113 and FL118 treatment and analyzed relevant gene expression by Western blots. We found that consistent with the different *in vivo* antitumor activity between FL118 and FL113 (Figure 2), FL118 was much more effective in inhibiting relevant gene expression *in vivo* as well

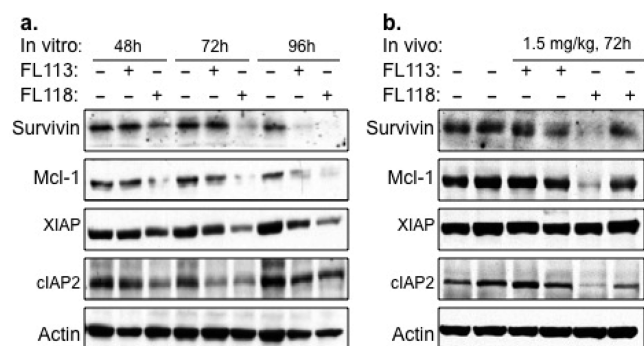


Figure 4. Effects of FL113 and FL118 on the expression of survivin, Mcl-1, XIAP, and cIAP2: (a) Subconfluent human head-and-neck FaDu cancer cells were treated with or without FL113 (10 nM) or FL118 (10 nM) for 48, 72, and 96 h. Cells were then lysed and analyzed by Western blots using antibodies for survivin, Mcl-1, XIAP, or cIAP2. Actin is the internal control for total protein loading. (b) Human head-and-neck FaDu cancer cell-derived xenograft tumors were isolated from SCID mice with or without FL113 or FL118 treatment for 72 h (one time i.p. injection, 1.5 mg/kg). The isolated tumors were then lysed using a motor-driven homogenizer and analyzed by Western blots with antibodies for survivin, Mcl-1, XIAP, cIAP2, or actin (internal control for total protein loading). Results from two independent tumors from two mice are shown in parallel.

(Figure 4b). Interestingly, while FL118 was shown to inhibit XIAP in cultured cancer cells, FL118 exhibited no inhibitory effect on XIAP from the *in vivo* tumor tissues (Figure 4b). This is an intriguing observation and would be worthy of further

investigation to determine whether this is a cancer cell type-specific phenomenon or evidence that the results derived from *in vitro* studies may not be fully consistent with the results derived from the *in vivo* studies. Alternatively, downregulation of XIAP *in vivo* may need a much longer time. Nevertheless, based on previous studies in the literature, we know that, while multiple antiapoptotic proteins from the IAP and Bcl-2 families (e.g., survivin, Mcl-1, XIAP, or cIAP2) could be simultaneously expressed in cancer, the essential role of these individual molecules in cancer initiation and development can be cancer type- and/or individual cancer patient-dependent. To induce cancer cell death, in many cases, it is unnecessary to inhibit the expression of all these antiapoptotic proteins for cancer cell apoptosis.

We would like to point out a differential level of inhibition in survivin and Mcl-1 expression between the two tumor tissue samples at 72 h following FL118 treatment (Figure 4b). This variation is consistent with the variation observed during the *in vivo* tumor regression shown in Figure 3. While most tumors regressed, some tumors were only inhibited (Figure 3). Therefore, the variation in FL118 target inhibition and tumor regression could be due to the distinct interaction between tumor and individual mice. This may result in such as vascular density differences between tumors and individual mice. Further studies are required to explore this phenomenon.

Finally, computational molecular modeling of the physical interaction of FL118 with the survivin X-ray crystal structure (PDB ID: 1F3H, 2.58 Å resolution) using SYBYL-X software package (Tripos, Inc., St. Louis, MO) indicated that FL118 forms several hydrogen bonds with survivin. However, using tritium-labeled FL118 (H^3 -FL118, Moravek Biochemicals) as a probe to hybridize the ProtoArray that displays over 9000 proteins (Invitrogen), we failed to find a physical interaction of FL118 with the human survivin protein. Of course, for many reasons, the FL118-survivin interaction could be missed in this protein array experiment. This includes but may not be limited to the fact that the affinity between FL118 and survivin is too low (i.e., $K_d > \mu M$); FL118 may only recognize the survivin protein when survivin is within a protein complex associated with other proteins, and/or the survivin protein may be in an unrecognizable confirmation on the ProtoArray surface. Therefore, studies are required in the future to explore this interesting area.

3.4. Alternative Demonstration of a Role of Survivin and Mcl-1 in FL118-Mediated Cancer Cell Growth Inhibition and Cell Death. Previously, we demonstrated that silencing of survivin by survivin-specific shRNA significantly increases FL118-mediated cancer cell growth inhibition and apoptosis induction (increased Annexin V staining).¹⁴ Similarly, shRNA knockdown of Mcl-1 expression significantly increased FL118-mediated PARP cleavage, a hallmark of apoptosis,¹⁴ while overexpression of XIAP or cIAP2 decreases PARP cleavage, caspase 3 activation, and Annexin V staining,¹⁴ suggesting these gene products play a role in FL118 function. Here, we generated a Tet-on controlled, doxycycline (Dox)-inducible survivin expression system (Figure 5a). Using this system we demonstrated that induction of survivin expression by Dox in the tumorigenic L929 fibrosarcoma cells significantly increases L929 cell resistance to FL118-induced growth inhibition in comparison with L929 cells without Dox induction (Figure 5b). Induction of survivin expression by Dox also significantly blocked FL118-mediated DNA fragmentation-induced cell death (Figure 5c). Similarly, forced expression of pcDNA3-Mcl-1 in H2122 lung cancer cells increased cell resistance to

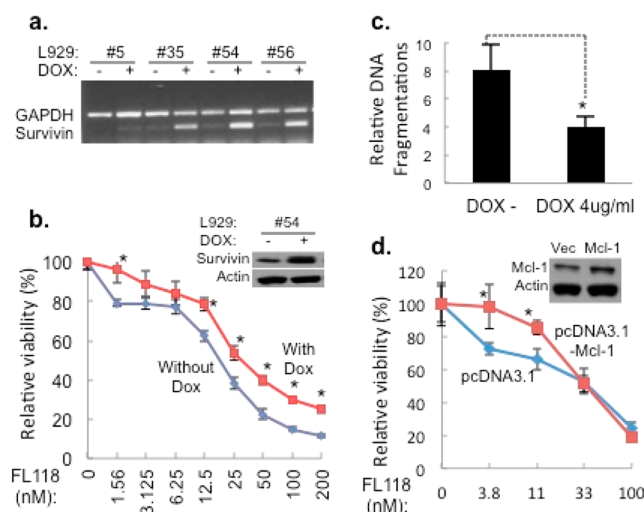


Figure 5. Role of survivin and Mcl-1 in FL118-mediated cancer cell growth inhibition and cell death: (a) Semiquantitative RT-PCR (semiQPCR) shows representative Tet-on induced survivin expression cell clones. The process of generation of individual cell clones with Tet-on controlled/Dox-inducible expression of survivin in tumorigenic L929 fibrosarcoma cells was described in the Experimental Section. Cell clones were induced with 4 $\mu g/mL$ Dox for 48 h; survivin mRNA expression was determined by semiQPCR and displayed on 1% agarose gels. GAPDH mRNA expression was used as an internal control during semiQPCR. (b) Induction of survivin expression by Dox protects L929 cells from FL118-mediated growth inhibition. The Western blot insert shows survivin protein induction by Dox (the insert in b). L929#54 cells were induced with and without Dox at 4 $\mu g/mL$ for 48 h and then treated with FL118 in a series of concentrations as indicated in the presence and absence of Dox for 72 h. Cell viability was determined by MTT assay. (c) Induction of survivin expression by Dox protects L929 cells from FL118-mediated cell death. L929#54 cells were induced with and without Dox at 4 $\mu g/mL$ for 48 h and then treated with 100 nM FL118 in the presence and absence of Dox for 72 h. The DNA fragmentation-induced cell death was determined by the DNA fragmentation cell death ELISA (Roche). (d) Forced expression of Mcl-1 in H2122 lung cancer cells protects cells from FL118-mediated growth inhibition in a limited range of FL118 concentrations. H2122 cells were transiently transfected with pcDNA3.1 control vectors or with pcDNA3.1-Mcl-1 expression vectors for 16 h. The transfected cells were then treated with different concentrations of FL118 as indicated for 72 h. The cell viability was then determined by MTT assay. The Western blot insert shows survivin protein expression in Mcl-1 transfected and untransfected H2122 lung cancer cells at the 48 h time point. *, represents the p -value < 0.05.

FL118-induced cell growth inhibition in comparison with pcDNA3.1 control vector transfected cells (Figure 5d). These data alternatively confirmed that survivin and Mcl-1 play a role in FL118 function and are downstream targets of FL118. Of note, we found that the L929 cell line is good for obtaining a Tet-on controlled survivin induction system and that the H2122 cell line is good for transient transfection of the pcDNA3.1-Mcl-1 expression vector.

3.5. Presence of a Free Hydroxyl Group (-OH) in the Lactone Ring of FL118 and FL113 Is Critical for FL118 or FL113 To Show Superior Antitumor Efficacy. Based on the fact that both FL113 and FL118 showed stronger antitumor activity than irinotecan (Figure 2), it is appropriate to do a comparison among FL113- and FL118-derived analogs. We synthesized three FL113 derivatives and four FL118 derivatives by esterification of the hydroxyl group at the 20-position with

various substituted benzoic acids (Schemes 1 and 2). Then, we determined their ability to inhibit survivin promoter activity and cancer cell growth. Our results showed that most of these compounds exhibit the inhibition of survivin promoter-driven luciferase activity at a concentration of 1000 nM in 2008 ovarian cancer cells (Figure 6). Consistently, the inhibitory activity of the

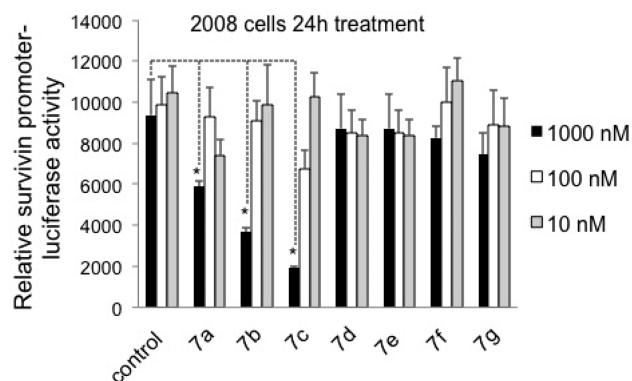


Figure 6. Effects of the seven derivatives of FL113 and FL118 on survivin promoter-driven luciferase activity: Ovarian cancer cells (2008) that stably express the survivin promoter-luciferase cassette at 50–70% subconfluence were treated with vehicle (control) or with one of the seven FL113 or FL118 derivatives at three concentrations as shown for 24 h. Cells were then lysed, followed by the luciferase activity assay as described in the Methods section. Data are presented in histograms, and each bar is the mean \pm SD (standard deviation) derived from three independent assays. The asterisk (*) denotes typical comparisons with p -value <0.05 .

pure S-configuration derivatives of **7b** and **7c** is higher than that of the mixture of R- and S-configuration derivatives, **7a**, **7f**, and **7g** (Figure 6). We further tested their potential to inhibit cell growth in three different cancer cell lines and found that similar to their ability to inhibit survivin promoter activity shown in Figure 6, most of these compounds at a concentration of 1000 nM could inhibit cancer cell growth (Figure 7). For the head and neck FaDu cell line, the inhibitory activity of **7a** to **7f** derivatives is higher than that of **7g**. For the colon HCT-8 cell line, the S-configuration **7b** is the most active compound among these seven compounds. However, these results (Figures 6 and 7) are about 1000 to 10,000 fold less effective than FL118.¹⁴ Next, we selected the compounds **7b** and **7c** to determine their antitumor activity in both head-and-neck (FaDu) and colon (SW620) tumors. The *in vivo* animal model experiments revealed that while these derivatives significantly decrease toxicity to animals (i.e., an increased MTD), they nearly lost antitumor activity (Figure 8a, b).

The initial idea for replacement of the hydrogen atom in the hydroxyl group with various small chemical groups was to generate new FL118 derivatives, with the hope of further decreasing toxicity to animals, without affecting antitumor activity by temporarily sealing the hydroxyl group during drug delivery. Although previous studies suggest that modification of the free hydroxyl group in camptothecin analogs via ester binds could be a promising way to improve *in vivo* antitumor activity and pharmacokinetic profile and reduce gastrointestinal toxicity,^{50–53} our studies with 20 O-linked benzoic acid ester derivatives of either FL118 or FL113 resulted in almost complete loss of antitumor activity *in vivo*, although toxicity was significantly lowered (MTD increased, Figure 8), and some of the FL113 and FL118 derivatives (e.g., **7a**, **7b**, **7c**) showed

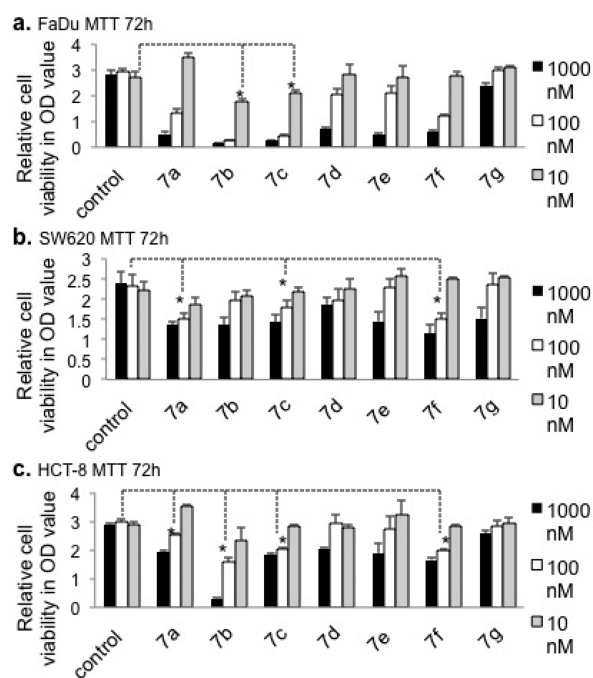


Figure 7. Effects of the seven derivatives derived from FL113 or FL118 on cancer cell growth: Three cancer cell lines (FaDu, SW620, HCT-8) as shown were used in this study. Cells at 50–70% subconfluence were treated with vehicle or with one of the seven FL113 or FL118 derivatives at three concentrations as shown for 72 h. Cell growth and viability were then determined by MTT assay. Data obtained from each cancer cell line were plotted as a histogram. Individual bars are the mean \pm SD (standard deviation) derived from independent assays ($N = 4$) in at least triplicates. (a) Results from the FaDu head and neck cancer cell line. (b) Results from the SW620 colon cancer cell line. (c) Results from the HCT-8 colon cancer cell line. The asterisk (*) denotes typical comparisons with p -value <0.05 .

inhibition of survivin promoter-luciferase activity and/or cell proliferation *in vitro* assay at the micromolar concentration level (Figures 6 and 7). The loss of antitumor activity for FL118 derivatives is likely due to the lack of appropriate hydrolytic enzymes to release the added chemical groups and restore the free hydroxyl group at position 20 of the FL118 molecule in animal models. This result suggests that the presence of a free hydroxyl group is important for FL118 to exhibit superior antitumor effects. In short, our studies are not fully consistent with the previous notion that modification of the free hydroxyl group in camptothecin or its analogues could improve *in vivo* antitumor activity and pharmacokinetic profile and reduce gastrointestinal toxicity.^{51–54} Our studies indicate that the overall decrease of toxicity (increased MTD) from position 20 FL118 derivatives could not override the loss of antitumor activity (Figure 8), suggesting FL118 is a unique core structure platform for generating novel analogues.

4. CONCLUSION

Based on our previous study of FL118, we conducted a follow-up study on the SAR of the hydroxyl group in the lactone ring of FL118. We found that the superior antitumor efficacy of FL118 heavily depends on both its primary structure and its steric configuration. FL118 exhibits a high ability to eradicate human tumors in animal models at doses even lower than its MTD. We synthesized seven position 20 esterifiable FL113 and FL118 derivatives and tested their *in vitro* and *in vivo* antitumor

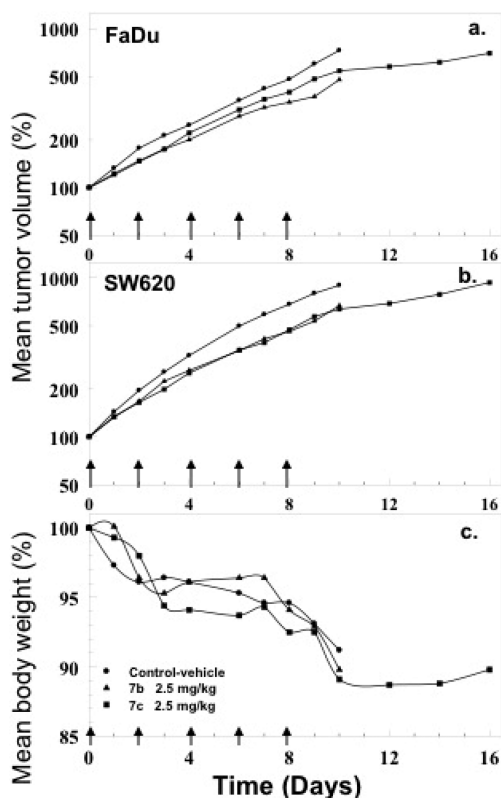


Figure 8. Antitumor activity and toxicity (body weight loss) of the selected two FL118 derivatives (7b, 7c) generated by replacement of the hydrogen atom of the hydroxyl group in the lactone ring of FL118. Treatment was initiated 7 days after xenograft tumor implantation (designated Day 0) at which time the tumor size is about 200–250 mm³. Treatment with the schedule of every other day for five times (q2 × 5) is indicated with arrows. (a and b) The mean tumor curves derived from five tumors on five mice treated with vehicle (control) or with one of the two FL118 derivatives (7b, 7c) for FaDu head and neck (a) or SW620 colon (b) tumors in SCID mouse models. The standard error (SE) of tumor variation is within 15% in the same group. (c) The mean mouse body weight curves derived from five mice treated with vehicle (control) or with one of the two FL118 derivatives (7b, 7c). Of note, the standard error (SE) of body weight loss variation is within 10% among each group.

activities. Although these new FL118 derivatives decrease the drug toxicity (increased MTD) to animals, they are about 1000 to 10,000 fold less effective than FL118. Therefore, overall, the presence of a free hydroxyl group is important for FL118 to exhibit superior antitumor effects. These findings narrow the window for further SAR studies on other potential chemical positions in the FL118 core structure molecule, which are currently being pursued by our research teams.

5. EXPERIMENTAL SECTION

5.1. Chemistry. **5.1.1. Materials and Methods Used.** All reagents used in the experiments were obtained from commercial sources and purified in a conventional manner. Published procedures were used for the preparation of 2-amino-4,5-methylenedioxybenzaldehyde (3), 20-S-10, 11-methylenedioxy-camptothecin (FL118), and 10,11-methylenedioxy-camptothecin (FL113).^{34–37} Thin-layer chromatography (TLC) was performed on Merck Silica Gel 60 F₂₅₄ plates. Flash column chromatography was performed on a silica gel (200–300 mesh; Qingdao Makall Group, Qingdao, China). Melting points were

measured on a WRX-1S melting-point apparatus and were uncorrected. ¹H NMR and ¹³C NMR spectra were taken on Jnm-Ecp-600 spectrometer (Jeol Ltd., Tokyo, Japan) with tetramethylsilane (Me₄Si) as the internal standard. Mass spectra were recorded on a Q-TOF Global mass spectrometer (Waters Co., Milford, MA, USA).

5.1.2. General Procedure for the Synthesis of Compounds 7a–7g. At room temperature, EDCI (423 mg, 2.21 mmol), DMAP (62 mg, 0.51 mmol), and substituted benzoic acid 6 (1.02 mmol) were added slowly to a stirring solution of FL113 or FL118 (100 mg, 0.255 mmol) in dry dichloromethane (60 mL), and then the resulting mixture suspension was heated to reflux under N₂ atmosphere for 12 h. After being cooled to room temperature, the mixture solution was then washed with 0.1 M HCl, water, and brine, and the organic layer was dried over anhydrous MgSO₄ for 12 h. After filtration to remove MgSO₄, the solvent was removed under reduced pressure. The residue was purified by flash chromatography on a silica gel (CH₂Cl₂/CH₃OH = 97/3, v/v) to yield the desired compound, 7a–7g, respectively.

5.1.3. 10,11-Methylenedioxy-camptothecin-20 (RS)-O-(4-bromobenzoate) (7a). The general synthetic method described above afforded 7a as yellow solid (42%), mp > 250 °C; ¹H NMR (DMSO-*d*₆, 600 MHz) δ: 8.44 (s, 1 H), 8.05 (d, *J* = 8.76 Hz, 2 H), 7.85 (d, *J* = 8.82 Hz, 2 H), 7.49 (s, 1 H), 7.43 (s, 1 H), 6.93 (s, 1 H), 6.25 (d, *J* = 4.44 Hz, 2 H), 5.55 (s, 2 H), 5.21 (s, 2 H), 2.31 (m, 2 H), 1.03 (t, *J* = 7.8 Hz, 3 H); ¹³C NMR (CF₃COOD, 150 MHz) δ: 171.4, 167.6, 158.7, 153.2, 148.3, 141.1, 140.1, 139.5, 139.2, 132.9, 131.7, 131.5, 129.8, 129.6, 125.6, 122.6, 105.4, 104.2, 102.5, 97.2, 77.4, 67.5, 54.6, 51.8, 31.7, 6.3; MS(ESI): *m/z*, 576.1 [M + H]⁺.

5.1.4. 10,11-Methylenedioxy-camptothecin-20 (S)-O-(4-iodobenzoate) (7b). The general synthetic method described above afforded 7b as yellow solid (56%), mp > 250 °C; ¹H NMR (DMSO-*d*₆, 600 MHz) δ: 8.45 (s, 1 H), 8.03 (d, *J* = 8.82 Hz, 2 H), 7.87 (d, *J* = 8.22 Hz, 2 H), 7.49 (s, 1 H), 7.44 (s, 1 H), 6.91 (s, 1 H), 6.25 (d, *J* = 4.38 Hz, 2 H), 5.55 (s, 2 H), 5.22 (s, 2 H), 2.30 (m, 2 H), 1.03 (t, *J* = 7.68 Hz, 3 H); ¹³C NMR (DMSO-*d*₆, 150 MHz) δ: 167.6, 164.6, 157.1, 151.9, 150.0, 149.2, 147.1, 146.9, 145.8, 138.8, 131.8, 130.8, 128.9, 128.1, 126.3, 118.4, 105.2, 103.9, 103.5, 103.0, 95.7, 77.1, 66.8, 49.1, 30.7, 8.3; MS(ESI): *m/z*, 623.4 [M + H]⁺.

5.1.5. 10,11-Methylenedioxy-camptothecin-20 (S)-O-(4-nitrobenzoate) (7c). The general synthetic method described above afforded 7c as yellow solid (31%), mp > 250 °C; ¹H NMR (CF₃COOD, 600 MHz) δ: 8.97 (s, 1 H), 8.42 (d, *J* = 8.82 Hz, 2 H), 8.35 (d, *J* = 8.76 Hz, 2 H), 7.74 (s, 1 H), 7.52 (s, 1 H), 7.46 (s, 1 H), 6.34 (s, 2 H), 5.98 (d, *J* = 18.18 Hz, 1 H), 5.69 (d, *J* = 17.04 Hz, 1 H), 5.68 (s, 2 H), 2.57 (m, 1 H), 2.45 (m, 1 H), 1.19 (t, *J* = 7.14 Hz, 3 H); ¹³C NMR (CF₃COOD, 150 MHz) δ: 170.7, 165.1, 158.4, 158.0, 152.9, 151.3, 147.5, 140.7, 139.9, 139.2, 138.9, 132.9, 131.3, 129.4, 129.3, 123.9, 122.5, 105.1, 103.8, 102.1, 96.9, 77.5, 67.2, 51.5, 31.4, 5.9; MS(ESI): *m/z*, 542.3 [M + H]⁺.

5.1.6. 10,11-Methylenedioxy-camptothecin-20 (S)-O-(3-bromobenzoate) (7d). The general synthetic method described above afforded 7d as yellow solid (58%), mp > 250 °C; ¹H NMR (DMSO-*d*₆, 600 MHz) δ: 8.45 (s, 1 H), 8.26 (s, 1 H), 8.12 (d, *J* = 8.22 Hz, 1 H), 8.01 (d, *J* = 7.68 Hz, 1 H), 7.60 (t, *J* = 7.74 Hz, 1 H), 7.49 (s, 1 H), 7.43 (s, 1 H), 6.99 (s, 1 H), 6.25 (d, *J* = 4.38 Hz, 2 H), 5.55 (s, 2 H), 5.22 (s, 2 H), 2.33 (m, 2 H), 1.03 (t, *J* = 7.2 Hz, 3 H); ¹³C NMR (DMSO-*d*₆, 150 MHz) δ: 167.6, 163.8, 157.1, 151.9, 150.2, 149.3, 147.2, 147.0, 145.7, 137.8, 132.6,

132.0, 130.9, 130.8, 129.4, 129.0, 126.3, 122.8, 118.5, 105.2, 103.7, 103.2, 94.3, 77.5, 66.9, 49.2, 30.7, 8.3; MS(ESI): m/z , 576.4 [M + H]⁺.

5.1.7. 10,11-Methylenedioxcamptothecin-20 (S)-O-(3-iodobenzoate) (7e). The general synthetic method described above afforded **7e** as yellow solid (62%), mp > 250 °C; ¹H NMR (DMSO-*d*₆, 600 MHz) δ: 8.45 (s, 1 H), 8.42 (s, 1 H), 8.16 (d, *J* = 8.28 Hz, 1 H), 8.12 (d, *J* = 7.74 Hz, 1 H), 7.48 (s, 1 H), 7.44 (t, *J* = 7.68 Hz, 2 H), 6.97 (s, 1 H), 6.26 (d, *J* = 4.44 Hz, 2 H), 5.76 (s, 2 H), 5.55 (s, 2 H), 2.33 (m, 2 H), 1.02 (t, *J* = 7.14 Hz, 3 H); ¹³C NMR (DMSO-*d*₆, 150 MHz) δ: 167.6, 163.7, 157.1, 151.9, 150.1, 149.3, 147.1, 147.0, 145.8, 143.6, 138.3, 131.8, 130.8, 129.6, 129.0, 126.2, 118.4, 105.2, 103.6, 103.1, 95.8, 94.3, 77.4, 66.9, 55.4, 50.8, 30.8, 8.3; MS(ESI): m/z , 623.0 [M + H]⁺.

5.1.8. 10,11-Methylenedioxcamptothecin-20 (RS)-O-(4-chlorobenzoate) (7f). The general synthetic method described above afforded **7f** as yellow solid (55%), mp > 250 °C; ¹H NMR (DMSO-*d*₆, 600 MHz) δ: 8.46 (s, 1 H), 8.14 (d, *J* = 8.82 Hz, 2 H), 7.72 (d, *J* = 8.82 Hz, 2 H), 7.49 (s, 1 H), 7.43 (s, 1 H), 6.93 (s, 1 H), 6.26 (d, *J* = 4.44 Hz, 2 H), 5.55 (s, 2 H), 5.23 (s, 2 H), 2.31 (m, 2 H), 1.03 (t, *J* = 7.68 Hz, 3 H); ¹³C NMR (DMSO-*d*₆, 150 MHz) δ: 167.6, 164.4, 157.1, 151.9, 150.1, 149.3, 147.2, 147.0, 145.8, 139.2, 132.1, 130.7, 129.9, 129.0, 127.5, 127.0, 118.4, 114.3, 106.4, 105.2, 103.6, 103.1, 77.2, 66.9, 50.8, 30.7, 8.3; MS(ESI): m/z , 531.1 [M + H]⁺.

5.1.9. 10,11-Methylenedioxcamptothecin-20 (RS)-O-(3,4-dimethoxybenzoate) (7g). The general synthetic method described above afforded **7g** as yellow solid (34%), mp > 250 °C; ¹H NMR (DMSO-*d*₆, 600 MHz) δ: 8.45 (s, 1 H), 7.81 (d, *J* = 9.9 Hz, 1 H), 7.50 (d, *J* = 4.2 Hz, 2 H), 7.44 (s, 1 H), 7.19 (d, *J* = 8.82 Hz, 1 H), 6.91 (s, 1 H), 6.26 (d, *J* = 3.3 Hz, 2 H), 5.54 (s, 2 H), 5.23 (s, 2 H), 3.88 (s, 3 H), 3.82 (s, 3 H), 2.29 (m, 2 H), 1.03 (t, *J* = 6.24 Hz, 3 H); ¹³C NMR (CF₃COOD, 150 MHz) δ: 171.6, 167.9, 158.6, 155.1, 153.2, 148.6, 148.5, 141.1, 140.1, 139.5, 139.1, 129.8, 129.5, 126.3, 122.5, 119.5, 112.8, 111.3, 105.4, 104.1, 102.6, 97.2, 77.2, 67.5, 55.4, 51.8, 31.7, 6.3; MS(ESI): m/z , 557.2 [M + H]⁺.

5.2. Biological Studies. **5.2.1. Reagents, Compounds, and Tumor Types Used.** Survivin antibody (FL-142) was purchased from Santa Cruz. Antibodies for Mcl-1, XIAP, and cIAP2 were purchased from Cell Signaling. Actin antibody (A2066) was purchased from Sigma. The pcDNA3.1 vector was purchased from Invitrogen. pcDNA3.1-Mcl-1 was purchased from Addgene (<http://www.addgene.org>). The Tet-on system and doxycycline (Dox) were purchased from Clontech.

Compounds used for cell culture studies were first dissolved in DMSO at a 1000× stock solution and then directly diluted for 1000× with cell culture medium to the finally needed concentration. The compounds used for the *in vivo* testing of antitumor activity and toxicity were formulated in the same recipe as previously reported by us.¹⁴

Human 11124 and 14528 colon cancer xenograft tumors were initially isolated from cancer patients at Roswell Park Cancer Institute (RPCI) and established in SCID (severe combined immunodeficient) mice. Human cancer cell line-derived tumor xenografts (human head and neck FaDu and human colon SW620) were established by subcutaneously injecting 1–3 million cultured cancer cells. The xenografts were passed through 1–3 generations by subtransplanting 40–50 mg non-necrotic tumor tissues via a trocar from the passage xenograft tumors. The derived xenograft tumors were used for *in vivo* experiments. Xenograft tumor mice for experiments were prepared using the same method as xenograft tumor passage.

5.2.2. Animal Models Used for Human Tumor Xenograft Experiments. Six to 12-week-old female athymic nude mice (nu/nu, body weight 20–25 g) were purchased from Charles River Laboratories International, Inc. (Wilmington, MA) or Harlan Sprague–Dawley Inc. (Indianapolis, IN). Six to 12-week-old female SCID mice were purchased from the RPCI Laboratory Animal Facility (LAR). Mice were housed at 5 mice per cage with water and food *ad libitum*. All animal experiments were performed in accordance with our IACUC (Institute Animal Care and Use Committee)-approved animal protocol.

5.2.3. Determination of the Maximum Tolerated Dose (MTD) for FL118 Analogues. In this study, we took advantage of the known MTD for FL118 reported previously¹⁴ as a start point by escalating with 0.5 mg/kg intervals until the MTD was achieved. Each dose was tested on a cohort of 5 mice in individual independent experiments. The MTD was defined as the highest drug dose at the defined drug administration schedule and route causing no drug-related lethality in mice with a body weight loss ≤20% of original body weight with reversible and temporary toxicities.

5.2.4. Documentation of Tumor Sizes and Anticancer Activity. During animal experiments, tumor size and animal body weight were documented daily during week days until the end of the experiments, or for the first 3 weeks and then every other day (Monday, Wednesday, and Friday) until the end of the experiments. Two dimensions (mm) of a tumor (*L*, longest axis; *W*, shortest axis) were measured with a Vernier caliper. Tumor volume (mm³) was estimated using the formula of “tumor volume (mm³) = 1/2(LW²)”. All figures were made using Sigma Plot software.

5.2.5. Cancer Cell Lines Used and Cell Culture. The human head and neck squamous cell carcinoma cell line FaDu, the human ileocecal adenocarcinoma (HCT-8), and colon cancer (SW620) cell lines were from American Type Culture Collection (ATCC, Manassas, VA). The human ovarian cancer cell line 2008 (a gift from Dr. Kunle Odunsi, Roswell Park Cancer Institute) was originally derived from a patient with ovary cystadenocarcinoma.⁵⁰ Tumorigenic L-929 fibrosarcoma cells were purchased from ATCC. H2122 lung cancer cells were from Dr. Daniel Chan (University of Colorado, Aurora) as a gift. Cells were grown either in RPMI 1640 medium (HCT-8, SW620, 2008, L929, H2122) or in Eagle’s minimum essential medium (FaDu), which were supplemented with 10% heat inactivated FCS, 100 U/mL of penicillin, and 0.1 μg/mL of streptomycin. Cells were cultured in a 5% CO₂ incubator at 37 °C and subcultured every 3–4 days. All cell lines were mycoplasma-free, confirmed by MycoSensor PCR Assay kit (Stratagene).

5.2.6. Immunoblotting Analysis (Western Blot). Western blots were performed as previously described.⁵⁵ Proteins of interest were detected using Western Lightning-ECL (Perkin-Elmer, Waltham, MA) and visualized by exposure for various times (5–60 s). Actin was used as an additional internal control for equal protein loading.

5.2.7. Generation of Tet-On-Controlled Survivin Expression in Tumorigenic L929 Fibrosarcoma Cells. Survivin cDNA was subcloned from pcDNA3-survivin expression vector into pTREhyg vector (Clontech) at BamH I and Sal I sites in the cis-direction to generate pTREhyg-survivin expression vector (hygromycin resistant). The pTREhyg-survivin vectors were then cotransfected with pTet-On vector (G418 resistant, Clontech) into the tumorigenic L929 fibrosarcoma cells. Transfected cells were grown in the presence of both G418 and hygromycin to select G418/hygromycin-resistant cell

clones. Each of the isolated G418/hygromycin-resistant cell clones was grown in the presence (to turn survivin on) and absence (to turn survivin off) of doxycycline (Dox) for 48 h, respectively. Survivin mRNA expression in individual cell clones was determined by semiquantitative RT-PCR (semiQPCR), followed by display of the PCR products on agarose gel (results from representative cell clones are shown in Figure 5a) as previously described.⁵⁶ The semiQPCR-identified positive cell clone that was used for experiments was further confirmed by Western blotting analysis (Figure 5b, insert).

5.2.8. MTT Assays. Cancer cell growth/viability was determined by a MTT assay.⁵⁶ MTT, a tetrazolium salt with the chemical definition of 3-[4,5-dimethylthiazol-2-yl]-2,5-diphenyltetrazolium bromide, was used as a colorimetric substrate for measuring cell viability. Seventy-two hours post treatment with vehicle or individual compounds, MTT was added to a final concentration of 0.5 mg/mL onto treated cells in 96-well plates. Cells were further incubated in a 5% CO₂ incubator at 37 °C for an additional 4 h and then lysed thoroughly with lysis buffer (20% SDS, 50% *N,N*-dimethylformamide, pH 4.7, 100 μ L/well). The absorbance in the relevant wells was measured at 570 nm using an Ultra Microplate Reader (Bio-Tek Instruments). The data derived from luciferase activity and MTT assays were analyzed using Excel 2010. Each bar is presented as mean \pm standard deviation (SD).

5.2.9. DNA Fragmentation Cell Death ELISA Assays. Tet-on survivin L929 cells were induced with Dox (4 μ g/mL) for 48 h and then treated with 50 nM FL118 for 72 h. Cells were then analyzed for DNA fragmentation-induced cell death determination using a Cell Death Detection ELISA^{plus} assay kit (Roche, Indianapolis, IN) following the recommended protocol as previously described.⁵⁶ Briefly, \sim 4000 Dox-induced and uninduced cells were seeded per well in a 96-well plate overnight and then treated with or without 50 nM FL118 for 72 h in the presence or absence of Dox. Cells were then lysed, and the lysates were cleared by centrifugation; the resulting supernatant was used for testing DNA fragmentation-induced cell death as previously described.⁵⁶

5.2.10. Luciferase Activity Assays. Luciferase activity assays were performed following the protocol described in our previously publications.^{57,58} Briefly, 2008 ovarian cancer cells that were stably transfected with the pLuc-4080 survivin promoter–luciferase construct were seeded and grown to a subconfluent state in 48 well plates. Cells were then treated with the defined concentration of drugs in triplicate for 24 h and then followed by processing of the luciferase assays using the PAE4550 Luciferase Reporter Assay System (Promega). Data were normalized to equal total protein amounts as arbitrary units to show relative promoter activity.

5.2.11. Statistical Analysis. The *p*-value was analyzed via an unpaired two-tailed student *t*-test assuming equal variance and set at the nominal level of 0.05 or less as significance. Individual time points represent the mean \pm standard deviation (SD, Figures 5, 6, and 7) or the mean \pm standard error (SE, Figures 2 and 8). The asterisk (*) represents the *p*-value < 0.05.

■ ASSOCIATED CONTENT

● Supporting Information

¹H NMR and ¹³C NMR spectra for new compounds. This material is available free of charge via the Internet at <http://pubs.acs.org>.

■ AUTHOR INFORMATION

Corresponding Authors

*E-mail: jiangtao@ouc.edu.cn. Tel.: 0086-532-82032712. Fax: 0086-532-82033054.

*E-mail: fengzhi.li@roswellpark.org. Tel.: (716)-845-4398. Fax: (716)-845-8857.

Author Contributions

J.Z., X. Ling, S.C., and X. Liu made equal contributions in this work.

Notes

The authors declare the following competing financial interest(s): FL118 will be further developed in Canget BioTekpharma Company (www.canget-biotek.com). F.L. is the founder of Canget, and F.L., X.L., X.J.L. and T.J. are initial investors in Canget.

■ ACKNOWLEDGMENTS

We would like to thank the Animal Center (DLAR) staff and attending veterinarians for daily care of our animals at RPCI and helping us to discover possible issues during our experiments. We also would like to thank Ms. Sumei Ren and Xiuli Zhang from the School of Pharmacy, Ocean University of China for their MS and NMR analysis. Additionally, we would like to thank other lab members from the Li and Jiang laboratories for being a part of our team and for their cooperation and support of these studies. We also would like to thank Editor David Hadbawnik of the English Department from the State University of New York (SUNY) at Buffalo (UB) for reading, correcting, and editing this manuscript. Finally, we sincerely thank Dr. Suzanne M. Hess (Research Support Services, Roswell Park Cancer Institute, Buffalo, NY) for critically reading and revision of this manuscript before publication. This work was sponsored in part by grants from Natural Science Foundation of China (NSF) (21171154) and a Special Fund for Marine Scientific Research in the Public Interest of China (201005024) to T.J.; by grants from US Army Department of Defense (PC110408), Mesothelioma Applied Research Foundation (Alexandria, VA), and the Roswell Park Alliance Foundation (Buffalo, NY) to F.L.; and by shared resources supported by NCI Cancer Center Core Support Grant to Roswell Park Cancer Institute (CA016056). Of note, S.C. was paid by grants in part from a grant to F.L. during this work.

■ REFERENCES

- (1) Yoon, M. J.; Park, S. S.; Kang, Y. J.; Kim, I. Y.; Lee, J. A.; Lee, J. S.; Kim, E. G.; Lee, C. W.; Choi, K. S. Aurora B confers cancer cell resistance to TRAIL-induced apoptosis via phosphorylation of survivin. *Carcinogenesis* **2012**, *33*, 492–500.
- (2) Okamoto, K.; Okamoto, I.; Hatashita, E.; Kuwata, K.; Yamaguchi, H.; Kita, A.; Yamanaka, K.; Ono, M.; Nakagawa, K. Overcoming erlotinib resistance in EGFR mutation-positive non-small cell lung cancer cells by targeting survivin. *Mol. Cancer Ther.* **2012**, *11*, 204–13.
- (3) Park, E.; Gang, E. J.; Hsieh, Y. T.; Schaefer, P.; Chae, S.; Klemm, L.; Huantes, S.; Loh, M.; Conway, E. M.; Kang, E. S.; Hoe Koo, H.; Hofmann, W. K.; Heisterkamp, N.; Pelus, L.; Keerthivasan, G.; Crispino, J.; Kahn, M.; Muschen, M.; Kim, Y. M. Targeting survivin overcomes drug resistance in acute lymphoblastic leukemia. *Blood* **2011**, *118*, 2191–9.
- (4) Trabulo, S.; Cardoso, A. M.; Santos-Ferreira, T.; Cardoso, A. L.; Simoes, S.; de Lima, M. C. P. Survivin Silencing as a Promising Strategy To Enhance the Sensitivity of Cancer Cells to Chemotherapeutic Agents. *Mol. Pharmaceutics* **2011**, *8*, 1120–1131.
- (5) Rahman, K. M. W.; Banerjee, S.; Ali, S.; Ahmad, A.; Wang, Z. W.; Kong, D. J.; Sakr, W. A. 3,3'-Diindolylmethane Enhances Taxotere-

Induced Apoptosis in Hormone-Refractory Prostate Cancer Cells through Survivin Down-regulation. *Cancer Res.* **2009**, *69*, 4468–4475.

(6) Li, F.; Ling, X. Survivin study: an update of “what is the next wave”? *J. Cell. Physiol.* **2006**, *208*, 476–86.

(7) Rodel, F.; Hoffmann, J.; Distel, L.; Herrmann, M.; Noisternig, T.; Papadopoulos, T.; Sauer, R.; Rodel, C. Survivin as a radioresistance factor, and prognostic and therapeutic target for radiotherapy in rectal cancer. *Cancer Res.* **2005**, *65*, 4881–4887.

(8) Carter, B. Z.; Mak, D. H.; Schober, W. D.; Cabreira-Hansen, M.; Beran, M.; McQueen, T.; Chen, W. J.; Andreeff, M. Regulation of survivin expression through Bcr-Abl/MAPK cascade: targeting survivin overcomes imatinib resistance and increases imatinib sensitivity in imatinib-responsive CML cells. *Blood* **2006**, *107*, 1555–1563.

(9) Wu, J.; Ling, X.; Pan, D.; Apontes, P.; Song, L.; Liang, P.; Altieri, D. C.; Beeraman, T.; Li, F. Molecular mechanism of inhibition of survivin transcription by the GC-rich sequence-selective DNA binding antitumor agent, hedamycin: evidence of survivin down-regulation associated with drug sensitivity. *J. Biol. Chem.* **2005**, *280*, 9745–51.

(10) Saito, T.; Hama, S.; Izumi, H.; Yamasaki, F.; Kajiwara, Y.; Matsuura, S.; Morishima, K.; Hidaka, T.; Shrestha, P.; Sugiyama, K.; Kurisu, K. Centrosome amplification induced by survivin suppression enhances both chromosome instability and radiosensitivity in glioma cells. *Br. J. Cancer* **2008**, *98*, 345–55.

(11) Zhang, M.; Latham, D. E.; Delaney, M. A.; Chakravarti, A. Survivin mediates resistance to antiandrogen therapy in prostate cancer. *Oncogene* **2005**, *24*, 2474–82.

(12) Roca, H.; Varsos, Z.; Pienta, K. J. CCL2 protects prostate cancer PC3 cells from autophagic death via phosphatidylinositol 3-kinase/AKT-dependent survivin up-regulation. *J. Biol. Chem.* **2008**, *283*, 25057–73.

(13) Li, F. Compositions and Methods for Identifying Agents That Alter Expression of Survivin. WO Patent 2,008,073,201, 2008.

(14) Ling, X.; Cao, S.; Cheng, Q.; Keefe, J. T.; Rustum, Y. M.; Li, F. A novel small molecule FL118 that selectively inhibits survivin, Mcl-1, XIAP and cIAP2 in a p53-independent manner, shows superior antitumor activity. *PLoS One* **2012**, *7*, e45571.

(15) Burke, T. G.; Mishra, A. K.; Wani, M. C.; Wall, M. E. Lipid bilayer partitioning and stability of camptothecin drugs. *Biochemistry* **1993**, *32*, 5352–64.

(16) Vogler, M.; Walczak, H.; Stadel, D.; Haas, T. L.; Genze, F.; Jovanovic, M.; Gschwend, J. E.; Simmet, T.; Debatin, K. M.; Fulda, S. Targeting XIAP bypasses Bcl-2-mediated resistance to TRAIL and cooperates with TRAIL to suppress pancreatic cancer growth in vitro and in vivo. *Cancer Res.* **2008**, *68*, 7956–65.

(17) Ding, X.; Mohd, A. B.; Huang, Z.; Baba, T.; Bernardini, M. Q.; Lysterly, H. K.; Berchuck, A.; Murphy, S. K.; Buermeyer, A. B.; Devi, G. R. MLH1 expression sensitizes ovarian cancer cells to cell death mediated by XIAP inhibition. *Br. J. Cancer* **2009**, *101*, 269–77.

(18) Connolly, K.; Mitter, R.; Muir, M.; Jodrell, D.; Guichard, S. Stable XIAP knockdown clones of HCT116 colon cancer cells are more sensitive to TRAIL, taxanes and irradiation in vitro. *Cancer Chemother. Pharmacol.* **2009**, *64*, 307–16.

(19) Dai, Y.; Qiao, L.; Chan, K. W.; Zou, B.; Ma, J.; Lan, H. Y.; Gu, Q.; Li, Z.; Wang, Y.; Wong, B. L.; Wong, B. C. Loss of XIAP sensitizes rosiglitazone-induced growth inhibition of colon cancer in vivo. *Int. J. Cancer* **2008**, *122*, 2858–63.

(20) He, X.; Khurana, A.; Maguire, J. L.; Chien, J.; Shridhar, V. HtrA1 sensitizes ovarian cancer cells to cisplatin-induced cytotoxicity by targeting XIAP for degradation. *Int. J. Cancer* **2012**, *130*, 1029–35.

(21) Ndozangue-Tourigouine, O.; Sebbagh, M.; Merino, D.; Micheau, O.; Bertoglio, J.; Breard, J. A mitochondrial block and expression of XIAP lead to resistance to TRAIL-induced apoptosis during progression to metastasis of a colon carcinoma. *Oncogene* **2008**, *27*, 6012–22.

(22) Zhao, X.; Laver, T.; Hong, S. W.; Twitty, G. B., Jr.; Devos, A.; Devos, M.; Benveniste, E. N.; Nozell, S. E. An NF-kappaB p65-cIAP2 link is necessary for mediating resistance to TNF-alpha induced cell death in gliomas. *J. Neurooncol.* **2011**, *102*, 367–81.

(23) Miura, K.; Karasawa, H.; Sasaki, I. cIAP2 as a therapeutic target in colorectal cancer and other malignancies. *Expert Opin. Ther. Targets* **2009**, *13*, 1333–45.

(24) Shigemasa, K.; Katoh, O.; Shiroyama, Y.; Mihara, S.; Mukai, K.; Nagai, N.; Ohama, K. Increased MCL-1 expression is associated with poor prognosis in ovarian carcinomas. *Jpn. J. Cancer Res.: Gann* **2002**, *93*, 542–50.

(25) Takahashi, H.; Chen, M. C.; Pham, H.; Angst, E.; King, J. C.; Park, J.; Brovman, E. Y.; Ishiguro, H.; Harris, D. M.; Reber, H. A.; Hines, O. J.; Gukovskaya, A. S.; Go, V. L.; Eibl, G. Baicalein, a component of *Scutellaria baicalensis*, induces apoptosis by Mcl-1 down-regulation in human pancreatic cancer cells. *Biochim. Biophys. Acta* **2011**, *1813*, 1465–74.

(26) Simonin, K.; Brotin, E.; Dufort, S.; Dutoit, S.; Goux, D.; N'Diaye, M.; Denoyelle, C.; Gauduchon, P.; Poulain, L. Mcl-1 is an important determinant of the apoptotic response to the BH3-mimetic molecule HA14-1 in cisplatin-resistant ovarian carcinoma cells. *Mol. Cancer Ther.* **2009**, *8*, 3162–70.

(27) Mitchell, C.; Yacoub, A.; Hossein, H.; Martin, A. P.; Bareford, M. D.; Eulitt, P.; Yang, C.; Nephew, K. P.; Dent, P. Inhibition of MCL-1 in breast cancer cells promotes cell death in vitro and in vivo. *Cancer Biol. Ther.* **2010**, *10*, 903–17.

(28) Guoan, X.; Hanning, W.; Kaiyun, C.; Hao, L. Adenovirus-mediated siRNA targeting Mcl-1 gene increases radiosensitivity of pancreatic carcinoma cells in vitro and in vivo. *Surgery* **2010**, *147*, 553–61.

(29) Wei, S. H.; Dong, K.; Lin, F.; Wang, X.; Li, B.; Shen, J. J.; Zhang, Q.; Wang, R.; Zhang, H. Z. Inducing apoptosis and enhancing chemosensitivity to gemcitabine via RNA interference targeting Mcl-1 gene in pancreatic carcinoma cell. *Cancer Chemother. Pharmacol.* **2008**, *62*, 1055–64.

(30) Martin, A. P.; Miller, A.; Emad, L.; Rahmani, M.; Walker, T.; Mitchell, C.; Hagan, M. P.; Park, M. A.; Yacoub, A.; Fisher, P. B.; Grant, S.; Dent, P. Lapatinib resistance in HCT116 cells is mediated by elevated MCL-1 expression and decreased BAK activation and not by ERBB receptor kinase mutation. *Mol. Pharmacol.* **2008**, *74*, 807–22.

(31) Lee, M.; Lapham, A.; Brimmell, M.; Wilkinson, H.; Packham, G. Inhibition of proteasomal degradation of Mcl-1 by cobalt chloride suppresses cobalt chloride-induced apoptosis in HCT116 colorectal cancer cells. *Apoptosis* **2008**, *13*, 972–82.

(32) Ling, X.; Li, F. An intravenous (i.v.) route-compatible formulation of FL118, a survivin, Mcl-1, XIAP, and cIAP2 selective inhibitor, improves FL118 antitumor efficacy and therapeutic index (TI). *Am. J. Transl. Res.* **2013**, *5*, 139–54.

(33) Giovannella, B. C.; Hinz, H. R.; Kozielski, A. J.; Stehlin, J. S., Jr.; Silber, R.; Potmesil, M. Complete growth inhibition of human cancer xenografts in nude mice by treatment with 20-(S)-camptothecin. *Cancer Res.* **1991**, *51*, 3052–5.

(34) Pendrak, I.; Wittrock, R.; Kingsbury, W. D. Synthesis and Anti-Hsv Activity of Methyleneedioxy Mappicine Ketone Analogs. *J. Org. Chem.* **1995**, *60*, 2912–2915.

(35) Mahindroo, N.; Ahmed, Z.; Bhagat, A.; Bedi, K. L.; Khajuria, R. K.; Kapoor, V. K.; Mara, K. L. Synthesis and structure-activity relationships of vasicine analogues as bronchodilatory agents. *Med. Chem. Res.* **2005**, *14*, 347–368.

(36) Wall, M. E.; Wani, M. C.; Nicholas, A. W.; Manikumar, G.; Tele, C.; Moore, L.; Truesdale, A.; Leitner, P.; Besterman, J. M. Plant antitumor agents. 30. Synthesis and structure activity of novel camptothecin analogs. *J. Med. Chem.* **1993**, *36*, 2689–700.

(37) Bao, Y.; Zhang, L.; Chen, F. Synthesis of 5'-(S)-1,1-dioxolane-5-oxo-(5'-ethyl-5'-hydroxyl-2'-H,5'-H,6'-H-6-oxopyrano)-[3',4'-f]-Δ-(superscript 6(8))-tetrahydroindolizine. *Chin. J. Med. Chem.* **2008**, *4*, 263–267.

(38) Bristol, J. A.; Comins, D. L.; Davenport, R. W.; Kane, M. J.; Lyle, R. E.; Maloney, J. R.; Portlock, D. E.; Horwitz, S. B. Analogs of camptothecin. *J. Med. Chem.* **1975**, *18*, 535–537.

(39) Horwitz, M. S.; Horwitz, S. B. Intracellular degradation of HeLa and adenovirus type 2 DNA induced by camptothecin. *Biochem. Biophys. Res. Commun.* **1971**, *45*, 723–7.

- (40) Wu, R. S.; Kumar, A.; Warner, J. R. Ribosome Formation Is Blocked by Camptothecin, a Reversible Inhibitor of Rna Synthesis. *Proc. Natl. Acad. Sci. U.S.A.* **1971**, *68*, 3009.
- (41) Horwitz, S. B.; Chang, C. K.; Grollman, A. P. Studies on camptothecin. I. Effects of nucleic acid and protein synthesis. *Mol. Pharmacol.* **1971**, *7*, 632–44.
- (42) Hsiang, Y. H.; Hertzberg, R.; Hecht, S.; Liu, L. F. Camptothecin induces protein-linked DNA breaks via mammalian DNA topoisomerase I. *J. Biol. Chem.* **1985**, *260*, 14873–8.
- (43) Stewart, A. F.; Schutz, G. Camptothecin-induced in vivo topoisomerase I cleavages in the transcriptionally active tyrosine aminotransferase gene. *Cell* **1987**, *50*, 1109–17.
- (44) Andoh, T.; Ishii, K.; Suzuki, Y.; Ikegami, Y.; Kusunoki, Y.; Takemoto, Y.; Okada, K. Characterization of a mammalian mutant with a camptothecin-resistant DNA topoisomerase I. *Proc. Natl. Acad. Sci. U.S.A.* **1987**, *84*, 5565–9.
- (45) Barth, S. W.; Briviba, K.; Watzl, B.; Jager, N.; Marko, D.; Esselen, M. In vivo bioassay to detect irinotecan-stabilized DNA/topoisomerase I complexes in rats. *Biotechnol. J.* **2010**, *5*, 321–7.
- (46) Richter, S. N.; Nadai, M.; Palumbo, M.; Palu, G. Topoisomerase I involvement in schedule-dependent interaction between 5-fluoro-uracil and irinotecan in the treatment of colorectal cancer. *Cancer Chemother. Pharmacol.* **2009**, *64*, 199–200.
- (47) Horisberger, K.; Erben, P.; Muessle, B.; Woernle, C.; Stroebel, P.; Kaehler, G.; Wenz, F.; Hochhaus, A.; Post, S.; Willeke, F.; Hofheinz, R. D. Margit. Topoisomerase I expression correlates to response to neoadjuvant irinotecan-based chemoradiation in rectal cancer. *Anti-cancer Drugs* **2009**, *20*, 519–24.
- (48) Mathijssen, R. H.; Loos, W. J.; Verweij, J.; Sparreboom, A. Pharmacology of topoisomerase I inhibitors irinotecan (CPT-11) and topotecan. *Curr. Cancer Drug Targets* **2002**, *2*, 103–23.
- (49) Kostopoulos, I.; Karavasilis, V.; Karina, M.; Bobos, M.; Xiros, N.; Pentheroudakis, G.; Kafiri, G.; Papakostas, P.; Vrettou, E.; Fountzilias, G. Topoisomerase I but not thymidylate synthase is associated with improved outcome in patients with resected colorectal cancer treated with irinotecan containing adjuvant chemotherapy. *BMC Cancer* **2009**, *9*, 339.
- (50) DiSaia, P.; Sinkovics, J.; Rutledge, F.; Smith, J. Cell-mediated immunity to human malignant cells. A brief review and further studies with two gynecologic tumors. *Am. J. Obstet. Gynecol.* **1972**, *114*, 979–989.
- (51) Wadkins, R. M.; Potter, P. M.; Vladu, B.; Marty, J.; Mangold, G.; Weitman, S.; Manikumar, G.; Wani, M. C.; Wall, M. E.; Von Hoff, D. D. Water soluble 20(S)-glycinate esters of 10,11-methylenedioxycamptothecins are highly active against human breast cancer xenografts. *Cancer Res.* **1999**, *59*, 3424–8.
- (52) Lerchen, H. G.; Baumgarten, J.; von dem Bruch, K.; Lehmann, T. E.; Sperzel, M.; Kempka, G.; Fiebig, H. H. Design and optimization of 20-O-linked camptothecin glycoconjugates as anticancer agents. *J. Med. Chem.* **2001**, *44*, 4186–95.
- (53) Rose, W. C.; Marathe, P. H.; Jang, G. R.; Monticello, T. M.; Balasubramanian, B. N.; Long, B.; Fairchild, C. R.; Wall, M. E.; Wani, M. C. Novel fluoro-substituted camptothecins: in vivo antitumor activity, reduced gastrointestinal toxicity and pharmacokinetic characterization. *Cancer Chemother. Pharmacol.* **2006**, *58*, 73–85.
- (54) Cao, Z.; Harris, N.; Kozielski, A.; Vardeman, D.; Stehlin, J. S.; Giovanella, B. Alkyl esters of camptothecin and 9-nitrocamptothecin: synthesis, in vitro pharmacokinetics, toxicity, and antitumor activity. *J. Med. Chem.* **1998**, *41*, 31–7.
- (55) Ling, X.; Bernacki, R. J.; Brattain, M. G.; Li, F. Induction of survivin expression by taxol (paclitaxel) is an early event, which is independent of taxol-mediated G2/M arrest. *J. Biol. Chem.* **2004**, *279*, 15196–203.
- (56) Ling, X.; Yang, J.; Tan, D.; Ramnath, N.; Younis, T.; Bundy, B. N.; Slocum, H. K.; Yang, L.; Zhou, M.; Li, F. Differential expression of survivin-2B and survivin-DeltaEx3 is inversely associated with disease relapse and patient survival in non-small-cell lung cancer (NSCLC). *Lung Cancer* **2005**, *49*, 353–361.
- (57) Wu, J.; Ling, X.; Pan, D.; Apontes, P.; Song, L.; Liang, P.; Altieri, D. C.; Beerman, T.; Li, F. Molecular mechanism of inhibition of survivin transcription by the GC-rich sequence selective DNA-binding antitumor agent, hedamycin: evidence of survivin downregulation associated with drug sensitivity. *J. Biol. Chem.* **2005**, *280*, 9745–51.
- (58) Cheng, Q.; Ling, X.; Haller, A.; Nakahara, T.; Yamanaka, K.; Kita, A.; Koutoku, H.; Takeuchi, M.; Brattain, M. G.; Li, F. Suppression of survivin promoter activity by YM155 involves disruption of Sp1-DNA interaction in the survivin core promoter. *Int. J. Biochem. Mol. Biol.* **2012**, *3*, 179–97.